Paper:

Hu, G., Li, L. & Zhang, Y. (2019). Two-dimensional electron gas in piezotronic devices. *Nano Energy, 59*, 667-673.
http://dx.doi.org/10.1016/j.nanoen.2019.03.001

Accepted Manuscript

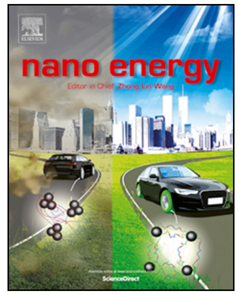

Two-dimensional electron gas in piezotronic devices

Gongwei Hu, Lijie Li, Yan Zhang

PII: S2211-2855(19)30189-2

DOI: https://doi.org/10.1016/j.nanoen.2019.03.001

Reference: NANOEN 3520

To appear in: *Nano Energy*

Received Date: 3 February 2019

Revised Date: 1 March 2019

Accepted Date: 1 March 2019

Please cite this article as: G. Hu, L. Li, Y. Zhang, Two-dimensional electron gas in piezotronic devices, *Nano Energy* (2019), doi: https://doi.org/10.1016/j.nanoen.2019.03.001.

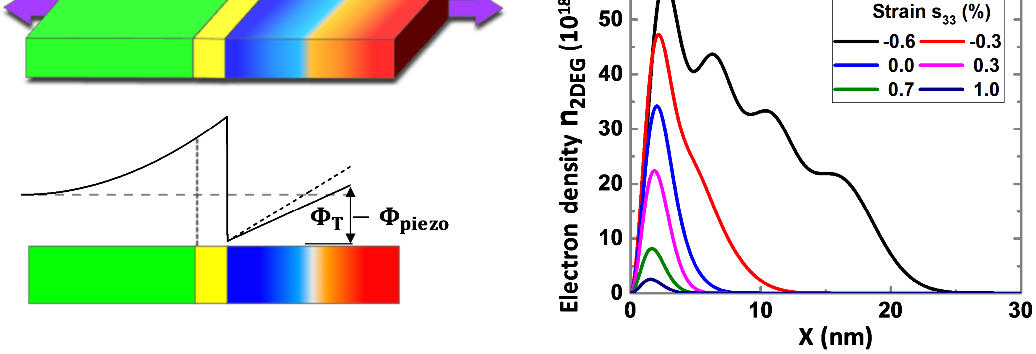

The two dimensional electron gas (2DEG) in AlGaN/GaN heterostructure has been investigated under various strain-induced piezoelectric fields. Quantum state can be effectively modulated by a perpendicular piezoelectric field. Piezotronic effect can be used for enhancing infrared photoelectric detection.

[1] *School of Physics, University of Electronic Science and Technology of China, Chengdu 610054, China*

[2] *Multidisciplinary Nanotechnology Centre, College of Engineering, Swansea University, Swansea, SA1 8EN, UK*

[3] *Beijing Institute of Nanoenergy and Nanosystems, Chinese Academy of Sciences, Beijing 100083, China*

[4] *College of Nanoscience and Technology, University of Chinese Academy of Sciences, Beijing 100049, China*

*To whom correspondence should be addressed, E-mail: L.Li@swansea.ac.uk and zhangyan@uestc.edu.cn

Abstract

Recent developments of piezotronic devices start to focus on the quantum behaviors of the nanostructured system going beyond the conventional device applications. Piezotronic devices utilize piezoelectric field to control the charge carrier behaviors at the junction, contact or interface of piezoelectric semiconductor, such as ZnO, GaN, and two-dimensional materials. In this study, we theoretically investigate the piezoelectric field effect on two-dimensional electron gas (2DEG) in AlGaN/GaN heterostructure by employing an approximate triangular potential model. Basic electronic properties such as wave function, electronic energy, electronic density distribution and the width of potential well are explored under the influence of the externally applied strain. From the electronic density, bound state can be eliminated or created by properly changing the external strain, meaning the effective modulation of piezotronic effect on quantum states. The piezoelectric field in 2DEG system is perpendicular to the electronic transport, which has remarkable advantage over the parallel case in switching devices. Furthermore, piezoelectric modulation of intrasubband transition enriches the fundamental theory of piezo-photonics and provides guidance for designing strain-gated infrared devices.

1. Introduction

Much attention has recently been concentrated on piezotronic and piezo-phototronic devices based on piezoelectric semiconductor materials, such as ZnO, GaN, InN and CdS. Following closely the invention of nanogenerator [1-4], plenty of multifunctional electromechanical devices such as solar cells [5, 6], light-emitting diodes (LEDs) [7, 8], strain sensor [9] and piezotronic field effect transistor [10] remarkably broaden the application prospects of conventional semiconductor transistors. In the development of flexible electronic devices, taxel-addressable matrices and photon-strain sensor arrays have also been made significant progresses in their chip integration [7, 11]. Piezotronic analog-to-digital converters (ADC) based on strain-gated transistors can realize the conversion from mechanical stimulus to digital logic signal [12]. Piezotronic effect on the performance improvement of wavelength and luminescence is studied in ZnO nanowires, CdTe quantum dot and single-layered MoS_2 [13-16]. Furthermore, piezotronic transistors based on topological insulators have received extensive attentions in their high-performance device applications [17, 18].

Since the concept of modulation doping in AlGaAs/GaAs system was introduced by Dingle *et al* in 1979 [19], two-dimensional electron gas (2DEG) has been widely studied in the area of theory and experiment. Due to the properties of high electron density and high mobility, 2DEG has much crucial applications in field effect transistors (FET) for high-power, high-frequency and high-temperature applications [20, 21]. Ultrafast optical switches can be designed based on the inter-subband transition (ISBT) of 2DEG in AlN/GaN multiquantum wells [22-24]. Additionally, terahertz and infrared detectors have also been developed by using 2DEG based transistors such as Schottky diodes and splitting-gated FET [25, 26]. On other hand, 2DEG is also an important studying platform for many quantum behaviors such as quantum Hall effect [27], topological insulator [28, 29] and topological superconductors [30]. Electron flowing in inversion asymmetric 2DEG can induce spin current which is promising for spintronic devices and quantum computing [31].

In this study, we take 2DEG in AlGaN/GaN heterostructure as a typical representative of perpendicular piezotronic modulation to explore the basic quantum properties and potential thin undoped AlGaN spacer layer sandwiched between an n-type AlGaN layer and a thick undoped GaN buffer [32]. The undoped AlGaN is used to reduce the scattering in 2DEG by the ionized impurities in n-type AlGaN layer [33]. Due to the spontaneous and piezoelectric polarization [24, 34, 35], the band structure is strongly bended by the sizable interfacial electric field. An approximate triangular potential well is then formed and high density 2DEG resides near the interface in GaN layer [36], as shown in Figure 1(a). Due to the piezoelectric property of GaN, tensile and compressive stress can produce additional piezoelectric polarization charges at the interface and weaken or enhance the interfacial electric field in triangular potential well, as illustrated in Figure 1(b) and (c). The carrier properties such as current-voltage characteristics, band structure and luminescence properties can be tuned and controlled by the piezoelectric field. The wave function, subband energy, the intrasubband transition energy, electron density and the width of potential well are investigated as the external applied strain varies. From the point view of electron density, the emergence of different bound state is significantly dependent on the external strain, demonstrating that quantum states in 2DEG can be controlled by piezotronic effect. Because the distribution width and total electron density in potential well is sensitive to the change of strain, the performance of the field effect transistor can be remarkably enhanced by perpendicular piezoelectric field. Distinguishing carrier recombination (happens in conduction electrons and valance holes) in piezo-phototronic effect, the tuning of piezoelectric field on intrasubband transition (for conduction electrons and carrier recombination) has potential applications in infrared detection.

2. Piezoelectric Field on 2DEG

Strain-induced piezoelectric field can be parallel or perpendicular to the direction of electric field produced by source-drain voltage. Parallel field is able to raise or reduce the barriers height along the carrier flowing direction and thus effectively control the carrier transport of nanodevices. Typical representatives include piezotronic p-n junction, metal-semiconductor (MS) contact and PIN diode [37, 38], which exhibit high performance of conducting channel is controlled by piezoelectric field and the ON/OFF current ratio is as high as 10^{10} which is much higher than those of parallel piezoelectric field cases. The conducting channel is formed by a thin layer two-dimensional electron gap (2DEG) near the interface of heterostructure.

Figure 2(a) shows the side view of AlGaN/GaN heterostructure and the conduction band structure. Because of the presence of the sizable interfacial electric field, amount of electrons are attracted to the interface and form a high concentration 2DEG region. The interfacial electric field is caused by the piezoelectric polarization charge (induced by lattice mismatch) and the spontaneous polarization [24, 34, 35]. Except for the above two polarization cases, applied strains can also produce piezoelectric charges at the interface and further modulate the quantum behaviors of 2DEG. By solving Schrödinger equation and Poisson equation [36], the wave function, subband energy, the intrasubband transition energy, distribution of electron density and the width of potential well are calculated by basic theory of quantum mechanics. The governing equations for describing 2DEG in AlGaN/GaN heterostructure are presented as follows.

The energy band can be controlled by strain-induced piezoelectric charges, which is the electrostatic effect governed by Poisson equation. For wurtzite structure semiconductor heterostructure AlGaN/GaN [39], Poisson equation is solved for the displacement field [32]

$$\frac{d}{dx}D(x)=\frac{d}{dx}\left[\varepsilon_s(x)F+P(x)\right]=q\left[p-n_{2DEG}+N_D^+-N_A^-+\rho_{piezo}\right] \tag{1}$$

where $D(x)$ is the displacement field, $\varepsilon_s(x)$ is the position-dependent dielectric constant, F is the electric field, $P(x)$ is the total polarization, p is the hole concentration, n_{2DEG} is the electron density of 2DEG, N_D^+ is the ionized donor concentration, N_A^- is the ionized acceptor concentration, ρ_{piezo} is the strain-induced piezo-charges concentration. The total polarization $P(x)$ is the sum of the spontaneous and (lattice mismatch) piezoelectric polarization [32].

Due to the presence of strong polarization field near the interface, the bending of equation [32, 36, 40, 41]. As an excellent approximation, triangular potential is commonly used to give the analytical results and presented as [36]

$$\phi(x)=\begin{cases}\infty & ,x=0\\ F_{piezo}x & ,x>0\end{cases} \tag{2}$$

where $\phi(x)$ is the potential distribution, F_{piezo} is the piezoelectric field. At the interface $x=0$, the electrostatic potential is assumed to be infinite height potential barrier due to the presence of larger band discontinuity [36, 41]. The electric field derives from piezoelectric polarization and spontaneous polarization in depletion region. Strong polarization field bends the band-edge profile, which can be considered as a quasi-triangular potential. Previous results have indicated that theoretical models based on triangular potential approximation are consistent with the experimental results for heterojunction devices, such as in Si inversion layer, AlGaAs/GaAs and AlGaN/GaN [36, 42, 43].

The piezoelectric field is tunable by the external applied strain. For three-dimensional bulk material [37, 44], piezoelectric field can be written as

$$F_{piezo}=F_0+\frac{q\rho_{piezo}W_{piezo}}{\varepsilon_{GaN}} \tag{3}$$

where F_0 is the intrinsic electric field without external strain, W_{piezo} is the width of piezo-charges distribution, ε_{GaN} is the dielectric constant of GaN.

Take one-band effective mass model as a typical example, we investigate piezotronic effect on 2DEG in wurtzite heterojunctions. Electron states in triangular potential well are described by Schrödinger equation

$$\frac{\hbar^2}{2m^*}\frac{d^2\psi}{dx^2}+\left(E-qF_{piezo}x\right)\psi=0, \tag{4}$$

where m^* is the electron effective mass of GaN. Solving equation (4) under the boundary condition: $\psi(0)=0$, $\psi(\infty)=0$, the energy levels and wave functions are given by [36]

$$\psi_k(x) = C \cdot A\left[\left(\frac{2m^*}{\hbar^2} qF_{piezo}\right)^{1/3} \left(x - \frac{E_k}{qF_{piezo}}\right)\right] \tag{6}$$

where $A(z) = 1/\pi \int_0^\infty cos\left(t^3/3 + zt\right)dt$ is Airy function and $C = 1\Big/\int_0^\infty A\left[\left(2m^* qF_s/\hbar^2\right)^{1/3}\left(x - E_k/qF_s\right)\right]dx$ is normalization factor. Once the basic quantum states are obtained, electron density of 2DEG can be calculated from

$$n_{2DEG}(x) = \sum_{k=1}^{M} \psi_k^*(x)\psi_k(x) \cdot n_k \tag{7}$$

where M is the number of bound states. n_k is the electron density occupied in *k*-th bound state

$$n_k = \frac{m^*}{\pi\hbar^2}\int_{E_k}^{\infty} \frac{1}{1+\exp\left[\left(E-E_F\right)/kT\right]} dE \tag{8}$$

where E_k is subband energy in the *k*-th bound state, E_F is the Fermi energy. The energy difference between two nearest subbands is obtained as

$$\Delta E_k = \pi qF_s\left(\frac{\hbar^2}{2m^*}\right)^{1/3}\left[\frac{3}{2}\pi qF_s\left(k+\frac{3}{4}\right)\right]^{-1/3} \tag{9}$$

The width of potential well can be evaluated by using the average distance of electron distribution in the *k*-th subband, which is defined by [36]

$$\left\langle X_k \right\rangle = \int_0^\infty x\psi_k^*(x)\psi_k(x)dx \tag{10}$$

For wurtzite structure GaN grown along *c*-axis [39], the piezoelectric coefficient is given by

$$(\mathbf{e})_{ijk} = \begin{pmatrix} 0 & 0 & 0 & 0 & e_{15} & 0 \\ 0 & 0 & 0 & e_{15} & 0 & 0 \\ e_{31} & e_{31} & e_{33} & 0 & 0 & 0 \end{pmatrix} \tag{11}$$

When only axis strain s_{33} is supplied, the piezoelectric polarization vector is written as [37]

$$P_z = e_{33}s_{33} = q\rho_{piezo}W_{piezo}\,. \tag{12}$$

In piezoelectric semiconductor devices, external applied strain induces the pure strain effect and the piezotronic effect. In this study, we consider the piezotronic effect and neglect the pure strain effect. The piezoelectric field can shift around 400 meV, and pure strain shift the conduction band-edge ~5 meV under the strain of 1.0% in AlGaN and GaN layer [45]. In addition, previous experimental and theoretical results show that the piezoelectric field in AlGaN/GaN heterojunction can reach over MV/cm [46, 47]. Therefore, the piezoelectric field can remarkably change the potential well structure and offer a strong piezotronic effect in AlGaN/GaN heterojunction.

For simplicity, the triangular potential approximation is used for clearly describing piezotornic effect on 2DEG. The self-consistent method can also be used for quantitative analysis of piezotronic device [41]. An initial trial electric potential $\phi(x)$ calculates the wavefunction and eigenenergies from Eq (4). The electron density of 2DEG n_{2DEG} is then obtained from Eq. (7) and Eq. (8), and further used to calculate a new electric potential $\phi(x)$. If the new electric potential is convergent to the old one, the obtained results are self-consistent. Otherwise, the iterative process will proceed until the convergence occurs.

The typical constant used in the calculation is presented as follow: The piezoelectric coefficient of GaN e_{33} is 0.65 C/m^2 [35], the dielectric constant ε_{GaN} is $10.4\varepsilon_0$ with the vacuum permittivity ε_0 [35], the effective electronic mass is $0.19m_0$ with the free electron mass m_0 [32], the temperature is 300 K, the width of piezo-charges distribution W_{piezo} is 0.25 nm [37], the intrinsic electric field F_0 without piezo-charges is 0.5 MV/cm [48], the Fermi energy E_F is 0.3 eV [24, 48].

The parameters for simulations are obtained from previous experimental works [49, 50], as shown in Table I. The *x*-axis is *c*-direction of wurtzite material. GaN and AlGaN layers are unintentionally doped and n-AlGaN layer is doped with shallow donors.

bound states with the energy lower than the Fermi energy. The 2DEG electron density n_{2DEG} is the summation over all subband electron density and localized in the potential well. The piezoelectric field F_{piezo} is linearly dependent on the external strain, as shown in Figure 2(b). For tensile stress (positive value strain s_{33}) supplied to GaN, the piezoelectric field is enhanced by strain-induced positive piezo-charges. Negative piezo-charges will weaken the piezoelectric field when the GaN endures compressive stress (negative value strain s_{33}). Wave function and corresponding energy eigenvalue are prerequisite to understand or obtain various quantum effects. Figure 2(c) plots the wave function of the lowest four bound states under strain varying from -0.6% to 1.0%. As the strain grows, the distribution of wave function becomes narrow and thus the electronic density distribution is increasingly concentrated at the interface. The shrinking of the distribution width is due to the increase of piezoelectric field which attracts more electrons close to the interface to screen the growing electric field. Additionally, for a fixed external strain the width of wave function distribution also gradually increases with the level of bound state. Figure 2(d) shows the subband energy of the lowest four states as a function of strain. Energy in different bound state decreases with the reducing of the strain and ends up to zero at the strain s_{33}=-0.7% where the piezoelectric field vanishes.

In order to give direct insight into piezotronic effect on electron states, the electron density of the lowest eight bound states is plotted in Figure 3(a). While the strain is low and close to -0.7%, electron density for different subbands becomes very high, which is mainly attributed to the vanishing piezoelectric field. In this case, the potential well is near flat and equivalent to unilaterally infinite depth potential well where almost all electrons are confined in the well. With the increasing of the strain, the electric field intensifies gradually and the potential well starts to decline. Electron density in high bound states reduces rapidly and ultimately becomes zero at a critical strain. This zero electron density can be viewed as the vanishing of quantum state (precisely speaking, quantum state always exists and cannot be existed in potential well which is the consequence of piezotronic effect. The critical strain from the ground state to the seventh bound state is 1.18%, 0.18%, -0.14%, -0.30%, -0.38%, -0.43%, -0.48% and -0.51%, respectively.

Figure 3(b) shows the total electron distribution of 2DEG in the potential well with the strain varying from -0.6% to 1.0%. Both the peak and width of electron density distribution increase with the strain decreasing, indicating that more and more electrons are populated on the well. Combining with the property of high mobility [51], high concentration electron gas in potential well leads to 2DEG being superior conductivity. Based on this principle, 2DEG is widely used in field effect transistor. In piezotronic field effect transistor, the formation of 2DEG is controlled by strain-induced piezoelectric field and ON/OFF switching ratio is 10^5-10^7 [52]. This ultrahigh switching ratio is attributed to the piezoelectric field which is perpendicular to the flowing direction of charge carriers and directly controls the opening and closure of the conducting channels in 2DEG, giving arise to excellent switching behavior. By contrast, those devices with piezoelectric field parallel to the transport direction, such as piezotronic p-n junction, metal-semiconductor contact and PIN diode is difficult to achieve high ON/OFF ratio due to the presence of tunneling current.

The energy transition between two intrasubbands in quantum dot or quantum well is usually related to the infrared photodetector [53-55]. Figure 4(a) plots the energy difference between two nearest subbbands as a function of strain. The breaking curve of energy difference is due to the consideration of the vanishing electron density of bound states in Figure 3(a). Energy difference decreases with the strain approaching to -0.7%. The first energy difference between the ground state and the first excited state is largest and has the critical strain greater than 0. As level of bound state increases, the breaking point decreases. When the applied strain is larger than the breaking point, the electron density vanishes and thus this energy transition is forbidden.

It should be noted that the bound states studied here are the conduction electron states and thus the energy transition between different states is intrasubband transition. As we can see from Figure 4(a), the transition energy varies in the order of 0.01 to 0.1 eV. However, for than the band gap of material which is the energy in interband transition between conduction electrons and valence holes. In piezo-photonics devices, light absorption or emission is based on the interband transition between electrons and holes, and thus the light frequency is higher. The tuning of piezoelectric field on intrasubband transition is a completely novel mechanism for mechanical-optical coupling devices, which broadens the fundamental theory of the piezo-photonics effect. Meanwhile, the light frequency of intrasubband transition in 2DEG is in infrared region which is much desired in infrared detector based on piezo-photonics effect.

Conventional AlGaAs/GaAs quantum well based far infrared photoelectric detectors use gate voltage to change wavelength [57]. Electric field induced by the gate voltage is limited to the level of ~100 KV/cm. Piezoelectric field can reach up to ~10 MV/cm, which is 100 times larger than the gate voltage induced field [46, 47]. As a result, wavelength can be effective adjusted by the piezoelectric field.

We also plot the average distribution width of the bound states as a function of strain in Figure 4(b). Similarly, there exists the breaking point in the curve owing to the vanishing electron density in bound states. The width sharply decreases when strain is closes to -0.7% and subsequently changes slowly. Ground state has the minimum width due to its low energy which is located at the bottom of triangular potential well.

In order for demonstrating the practical device application, we simulate the piezotronic transistor based on AlGaN/GaN heterojunction by the finite element method. The piezotronic device models including p-n junction, M-S junction, bipolar transistor and metal–insulator–semiconductor tunnel device have been simulated by using the COMSOL software package [37, 58, 59]. The structural parameters used in the AlGaN/GaN piezotronic transistor are displayed as following: the lengths of GaN, AlGaN and n-AlGaN are 20 nm, 1 nm and 40 nm, respectively. The dopant concentrations are 10^{14} cm^{-3}, 10^{14} cm^{-3} and 10^{17} cm^{-3}, and the cross-sectional area is set as 2 μm × 2 μm. Figure 5(a) shows I-V characteristics of the AlGaN/GaN piezotronic heterostructure with various strain-induce piezoelectric fields. The current significantly changes while the strain increases from -0.4% to 0.4%. Figure 5(b) shows an enhancement of the current when the strain increases from -0.4% to 0.4%,

5. Conclusions

We have theoretically studied the impact of piezotronic effect on 2DEG in AlGaN/GaN heterostructure. Using the approximation of triangular potential well, various electronic characteristics of 2DEG such as wave function, subband energy, band transition, electron density and the width of potential well are calculated under external applied strain. External strain can sensitively control electron density of bound states and even determine the appearance of bound state, directly demonstrating the piezotronic tuning of quantum states. Furthermore, we calculate the total electron concentration and effective distribution width of 2DEG which can remarkably enhance the switching performance of piezotronic field effect transistors due to the modulation of perpendicular piezoelectric field. Distinguishing the interband transition in conventional piezo-photonic devices, the intrasubband transition in 2DEG not only enriches the fundamental theory of piezo-photonics effect, but also offers a method for designing strain-gated infrared detecting devices.

Acknowledgement

The authors are thankful for the support from University of Electronic Science and Technology of China (ZYGX2015KYQD063), Swansea University, and SPARC II project.

312 (2006) 242-246.

[2] X. Wang, J. Song, J. Liu, Z.L. Wang, Direct-current nanogenerator driven by ultrasonic waves, Science, 316 (2007) 102-105.

[3] Y. Qin, X. Wang, Z.L. Wang, Microfibre-nanowire hybrid structure for energy scavenging, Nature, 451 (2008) 809-813.

[4] W.Z. Wu, Z.L. Wang, Piezotronics and piezo-phototronics for adaptive electronics and optoelectronics, Nat Rev Mater, 1 (2016).

[5] Y. Hu, Y. Zhang, Y. Chang, R.L. Snyder, Z.L. Wang, Optimizing the power output of a ZnO photocell by piezopotential, ACS nano, 4 (2010) 4220-4224.

[6] X. Wen, W. Wu, Z.L. Wang, Effective piezo-phototronic enhancement of solar cell performance by tuning material properties, Nano Energy, 2 (2013) 1093-1100.

[7] C.F. Pan, L. Dong, G. Zhu, S.M. Niu, R.M. Yu, Q. Yang, Y. Liu, Z.L. Wang, High-resolution electroluminescent imaging of pressure distribution using a piezoelectric nanowire LED array, Nat Photonics, 7 (2013) 752-758.

[8] C. Wang, R. Bao, K. Zhao, T. Zhang, L. Dong, C. Pan, Enhanced emission intensity of vertical aligned flexible ZnO nanowire/p-polymer hybridized LED array by piezo-phototronic effect, Nano Energy, 14 (2015) 364-371.

[9] J. Zhou, Y. Gu, P. Fei, W. Mai, Y. Gao, R. Yang, G. Bao, Z.L. Wang, Flexible piezotronic strain sensor, Nano Lett, 8 (2008) 3035-3040.

[10] X. Wang, J. Zhou, J. Song, J. Liu, N. Xu, Z.L. Wang, Piezoelectric field effect transistor and nanoforce sensor based on a single ZnO nanowire, Nano Lett, 6 (2006) 2768-2772.

[11] W. Wu, X. Wen, Z.L. Wang, Taxel-addressable matrix of vertical-nanowire piezotronic transistors for active and adaptive tactile imaging, Science, 340 (2013) 952-957.

[12] J.H. Nie, G.W. Hu, L.J. Li, Y. Zhang, Piezotronic analog-to-digital converters based on strain-gated transistors, Nano Energy, 46 (2018) 423-427.

[13] Y. Zhang, L.J. Li, Piezophototronic effect enhanced luminescence of zinc oxide nanowires, Nano Energy, 22 (2016) 533-538.

[14] L.J. Li, Y. Zhang, Simulation of wavelength selection using ZnO nanowires array, J Appl Phys, 121 (2017).

[15] L.J. Li, Y. Zhang, Controlling the luminescence of monolayer MoS2 based on the piezoelectric effect, Nano Res, 10 (2017) 2527-2534.

[16] Y. Zhang, J. Nie, L. Li, Piezotronic effect on the luminescence of quantum dots for micro/nano-newton force measurement, Nano Res, 11 (2018) 1977-1986.

[17] M.J. Dan, G.W. Hu, L.J. Li, Y. Zhang, High performance piezotronic logic nanodevices based on GaN/InN/GaN topological insulator, Nano Energy, 50 (2018) 544-551.

[18] G. Hu, Y. Zhang, L. Li, Z.L. Wang, Piezotronic Transistor Based on Topological Insulators, ACS nano, 12 (2018) 779-785.

[19] R. Dingle, H.L. Störmer, A.C. Gossard, W. Wiegmann, Electron mobilities in modulation‐doped semiconductor heterojunction superlattices, Applied Physics Letters, 33 (1978) 665-667.

[20] T.P. Chow, R. Tyagi, Wide Bandgap Compound Semiconductors for Superior High-Voltage Unipolar

intersubband transition in AlGaN/GaN quantum wells, Japanese Journal of Applied Physics Part 2-Letters & Express Letters, 36 (1997) L1006-L1008.

[23] N. Suzuki, N. Iizuka, Electron scattering rates in AlGaN/GaN quantum wells for 1.55-mu m inter-subband transition, Jpn J Appl Phys 2, 37 (1998) L369-L371.

[24] N. Suzuki, N. Iizuka, Effect of polarization field on intersubband transition in AlGaN/GaN quantum wells, Jpn J Appl Phys 2, 38 (1999) L363-L365.

[25] M.I. Dyakonov, M.S. Shur, Plasma wave electronics: Novel terahertz devices using two dimensional electron fluid, Ieee T Electron Dev, 43 (1996) 1640-1645.

[26] G. Cywinski, P. Sai, I. Yahniuk, P. Kruszewski, B. Grzywacz, J. Przybytek, P. Prystawko, A. Khachapuridze, K. Nowakowski-Szkudlarek, W. Knap, P. Wisniewski, B. Stonio, G.S. Simin, S.L. Rumyantsev, Towards resonant THz detector: Devices based on Schottky diodes to 2DEG GaN/AlGaN, DOI 10.23919/mikon.2018.8405335(2018) 715-718.

[27] B.J. van Wees, H. van Houten, C.W. Beenakker, J.G. Williamson, L.P. Kouwenhoven, D. van der Marel, C.T. Foxon, Quantized conductance of point contacts in a two-dimensional electron gas, Physical review letters, 60 (1988) 848-850.

[28] B.A. Bernevig, T.L. Hughes, S.C. Zhang, Quantum spin Hall effect and topological phase transition in HgTe quantum wells, Science, 314 (2006) 1757-1761.

[29] M. Konig, S. Wiedmann, C. Brune, A. Roth, H. Buhmann, L.W. Molenkamp, X.L. Qi, S.C. Zhang, Quantum spin hall insulator state in HgTe quantum wells, Science, 318 (2007) 766-770.

[30] B.S. Joon Sue Lee, Mihir Pendharkar, Anthony P. McFadden, Younghyun Kim, Henri J. Suominen, Morten Kjaergaard, Fabrizio Nichele, Charles M. Marcus, Chris J. Palmstrøm, Transport studies of epi-Al/InAs 2DEG systems for required building-blocks in topological superconductor networks, DOI arXiv:1703.03699(2017).

[31] Q. Song, H.R. Zhang, T. Su, W. Yuan, Y.Y. Chen, W.Y. Xing, J. Shi, J.R. Sun, W. Han, Observation of inverse Edelstein effect in Rashba-split 2DEG between SrTiO3 and LaAlO3 at room temperature, Science advances, 3 (2017).

[32] F. Sacconi, A. Di Carlo, P. Lugli, H. Morkoc, Spontaneous and piezoelectric polarization effects on the output characteristics of AlGaN/GaN heterojunction modulation doped FETs, Ieee T Electron Dev, 48 (2001) 450-457.

[33] D. Delagebeaudeuf, N.T. Linh, Metal-(n) AlGaAs-GaAs two-dimensional electron gas FET, Ieee T Electron Dev, 29 (1982) 955-960.

[34] O. Ambacher, J. Smart, J.R. Shealy, N.G. Weimann, K. Chu, M. Murphy, W.J. Schaff, L.F. Eastman, R. Dimitrov, L. Wittmer, M. Stutzmann, W. Rieger, J. Hilsenbeck, Two-dimensional electron gases induced by spontaneous and piezoelectric polarization charges in N- and Ga-face AlGaN/GaN heterostructures, J Appl Phys, 85 (1999) 3222-3233.

[35] O. Ambacher, B. Foutz, J. Smart, J.R. Shealy, N.G. Weimann, K. Chu, M. Murphy, A.J. Sierakowski, W.J. Schaff, L.F. Eastman, R. Dimitrov, A. Mitchell, M. Stutzmann, Two dimensional electron gases induced by spontaneous and piezoelectric polarization in undoped and doped AlGaN/GaN heterostructures, J Appl Phys, 87 (2000) 334-344.

[36] F. Stern, Self-Consistent Results forn-Type Si Inversion Layers, Phys Rev B, 5 (1972) 4891-4899.

III-V nitrides, Physical Review B, 56 (1997) 10024-10027.

[40] l. Ma, y. Wang, Z. Yu, l. Tian, Self-consistent numerical model and optimization of two-dimensional electron gases for AlGaN/GaN HEMT, DOI 10.1109/iwjt.2004.1306791(2004) 190-193.

[41] I.H. Tan, G.L. Snider, L.D. Chang, E.L. Hu, A self‐consistent solution of Schrödinger‐Poisson equations using a nonuniform mesh, J Appl Phys, 68 (1990) 4071-4076.

[42] H.K. Kwon, C.J. Eiting, D.J.H. Lambert, B.S. Shelton, M.M. Wong, T.G. Zhu, R.D. Dupuis, Radiative recombination of two-dimensional electrons in a modulation-doped Al0.37Ga0.63N/GaN single heterostructure, Appl Phys Lett, 75 (1999) 2788-2790.

[43] Y.R. Yuan, M.A.A. Pudensi, G.A. Vawter, J.L. Merz, New photoluminescence effects of carrier confinement at an AlGaAs/GaAs heterojunction interface, J Appl Phys, 58 (1985) 397-403.

[44] Y. Zhang, Z.L. Wang, Theory of piezo-phototronics for light-emitting diodes, Adv Mater, 24 (2012) 4712-4718.

[45] S.L. Chuang, Optical gain of strained wurtzite GaN quantum-well lasers, IEEE Journal of Quantum Electronics, 32 (1996) 1791-1800.

[46] N. Grandjean, B. Damilano, S. Dalmasso, M. Leroux, M. Laugt, J. Massies, Built-in electric-field effects in wurtzite AlGaN/GaN quantum wells, J Appl Phys, 86 (1999) 3714-3720.

[47] R. Langer, J. Simon, V. Ortiz, N.T. Pelekanos, A. Barski, R. Andre, M. Godlewski, Giant electric fields in unstrained GaN single quantum wells, Appl Phys Lett, 74 (1999) 3827-3829.

[48] S.F. Chichibu, A.C. Abare, M.S. Minsky, S. Keller, S.B. Fleischer, J.E. Bowers, E. Hu, U.K. Mishra, L.A. Coldren, S.P. DenBaars, T. Sota, Effective band gap inhomogeneity and piezoelectric field in InGaN/GaN multiquantum well structures, Applied Physics Letters, 73 (1998) 2006-2008.

[49] F. Stengel, S.N. Mohammad, H. Morkoç, Theoretical investigation of electrical characteristics of AlGaN/GaN modulation doped field‐effect transistors, J Appl Phys, 80 (1996) 3031-3042.

[50] E. Frayssinet, W. Knap, P. Lorenzini, N. Grandjean, J. Massies, C. Skierbiszewski, T. Suski, I. Grzegory, S. Porowski, G. Simin, X. Hu, M.A. Khan, M.S. Shur, R. Gaska, D. Maude, High electron mobility in AlGaN/GaN heterostructures grown on bulk GaN substrates, Appl Phys Lett, 77 (2000) 2551-2553.

[51] C.R. Elsass, I.P. Smorchkova, B. Heying, E. Haus, P. Fini, K. Maranowski, J.P. Ibbetson, S. Keller, P.M. Petroff, S.P. DenBaars, U.K. Mishra, J.S. Speck, High mobility two-dimensional electron gas in AlGaN/GaN heterostructures grown by plasma-assisted molecular beam epitaxy, Appl Phys Lett, 74 (1999) 3528-3530.

[52] C. Opoku, A.S. Dahiya, C. Oshman, C. Daumont, F. Cayrel, G. Poulin-Vittrant, D. Alquier, N. Camara, Fabrication of high performance field-effect transistors and practical Schottky contacts using hydrothermal ZnO nanowires, Nanotechnology, 26 (2015).

[53] V. Ryzhii, I. Khmyrova, M. Ershov, T. Iizuka, Theory of an Intersubband Infrared Phototransistor with a Nonuniform Quantum-Well, Semicond Sci Tech, 10 (1995) 997-1001.

[54] V. Ryzhii, The theory of quantum-dot infrared phototransistors, Semicond Sci Tech, 11 (1996) 759-765.

[55] Z.H. An, J.C. Chen, T. Ueda, S. Komiyama, K. Hirakawa, Infrared phototransistor using capacitively coupled two-dimensional electron gas layers, Appl Phys Lett, 86 (2005).

devices, Journal of Physics D: Applied Physics, 51 (2018) 324006.
[59] P. Zhu, Z.M. Zhao, J.H. Nie, G.W. Hu, L.J. Li, Y. Zhang, Ultra-high sensitivity strain sensor based on piezotronic bipolar transistor, Nano Energy, 50 (2018) 744-749.

Gongwei Hu received his B.S. degree (2014) from China Three Gorges University and M.S. degree in Theoretical Physics (2017) from Lanzhou University. He is currently pursuing the Ph.D degree under the guidance of Professor Yan Zhang in School of Physics in UESTC. His research focuses on the field of functional nanostructures and their physics.

Lijie Li is a professor at Swansea University, UK. His research interests are design, modeling, fabrication, and characterization of MEMS, NEMS, sensors and actuators. He is Fellow of IET, and senior member of IEEE.

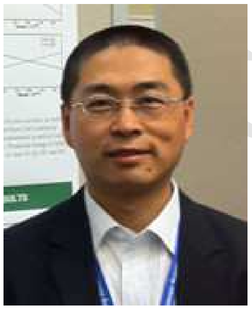

Yan Zhang is a professor at University of Electronic Science and Technology of China. He received his B. S. degree (1995) and Ph.D degree in Theoretical Physics (2004) from Lanzhou University. His research interests include self-powered nano/micro system, piezotronic and modeling of nonlinear dynamics of NEMS. He is senior member of IEEE.

Figure 1. Schematic of piezoelectric field on 2DEG in AlGaN/GaN quantum well and corresponding energy band diagram for (a) unstrained case, (b) stretched case and (c) compressed case. The height of the triangle potential well Φ_T is tunable by the piezoelectric potential Φ_{piezo}.

Figure 2. (a) Side view of AlGaN/GaN quantum well. Strain-induced piezo-charges is distributed at the interface. (b) Total piezoelectric field versus strain. (c) Wave function distribution for the first three subbands under different strains. (d) Subband energy as a function of strain.

Figure 3. (a) Electron density against strain for the different bound states; (b) Total electron density distribution of 2DEG in the potential well under different strains.

Figure 4. (a) The energy difference between two nearest intrasubbands as a function of strain; (b) the average distribution width of different bound states varying with strain. The appearance of the breaking point in the curves is due to the consideration of the vanishing bound state.

Figure 5. I-V characteristics of piezotronic transistior based on AlGaN/GaN heterojunction. (a) The current versus the voltage for the strain varying from -0.4% to 0.4%; (b) the current versus the strain under different applied voltages.

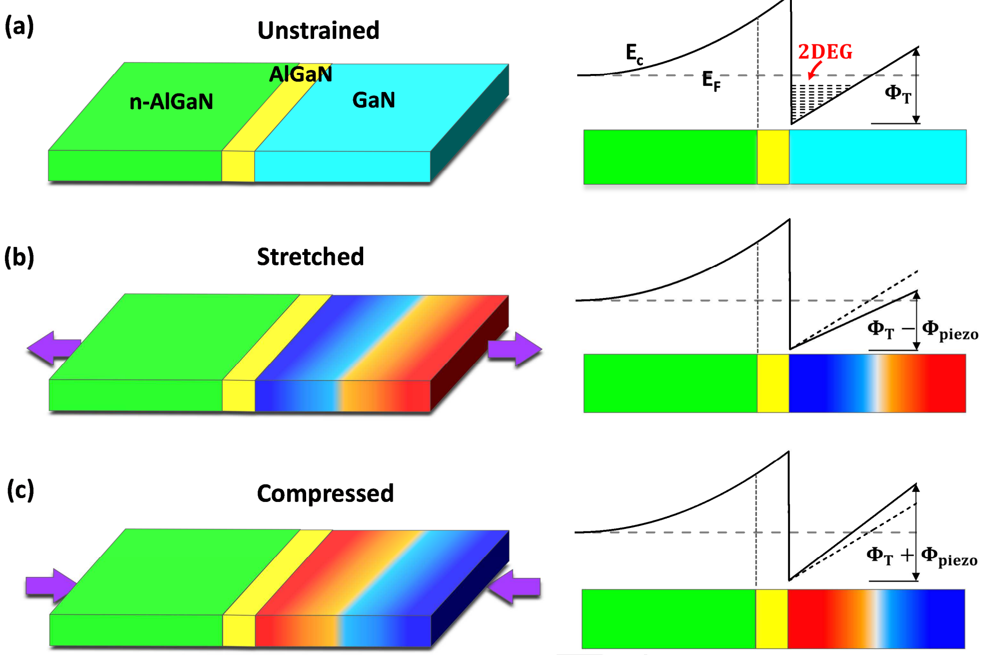

(a)
Unstrained
n-AlGaN
AlGaN
GaN
E_c
E_F
2DEG
Φ_T
(b)
Stretched
$\Phi_T - \Phi_{piezo}$
(c)
Compressed
$\Phi_T + \Phi_{piezo}$

Figure 1

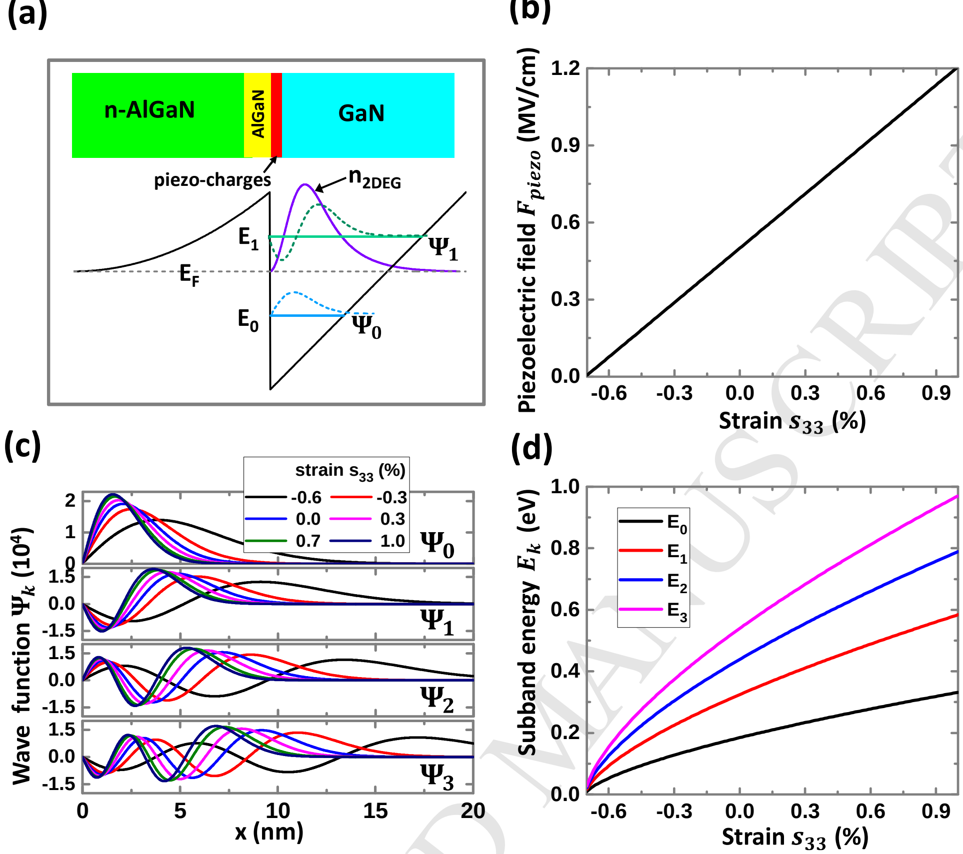

(a)
n-AlGaN
AlGaN
GaN
piezo-charges
n2DEG
E1
Ψ1
EF
E0
Ψ0
(b)
Piezoelectric field F_piezo (MV/cm)
Strain s33 (%)
(c)
strain s33 (%)
-0.6
-0.3
0.0
0.3
0.7
1.0
Ψ0
Ψ1
Ψ2
Ψ3
Wave function Ψk (10⁴)
x (nm)
(d)
E0
E1
E2
E3
Subband energy Ek (eV)
Strain s33 (%)

Figure 2

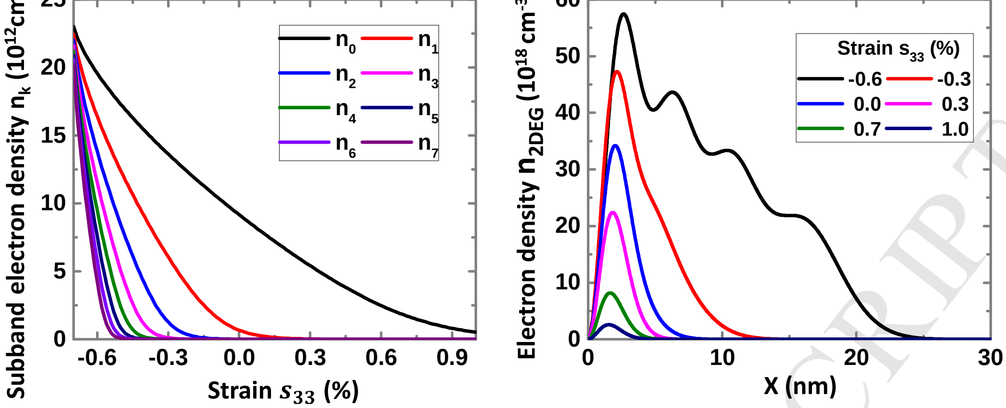

Subband electron density n_k (10^{12}cm
Strain s_{33} (%)
n_0
n_1
n_2
n_3
n_4
n_5
n_6
n_7
Electron density n_{2DEG} (10^{18} cm^{-3}
X (nm)
Strain s_{33} (%)
-0.6
-0.3
0.0
0.3
0.7
1.0

Figure 3

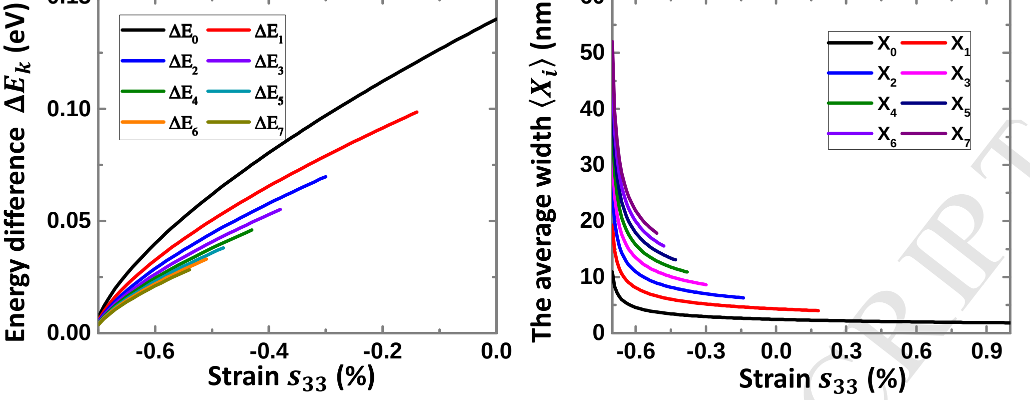
Energy difference ΔE_k (eV)
0.10
0.05
0.00
-0.6
-0.4
-0.2
0.0
Strain s_{33} (%)
ΔE_0
ΔE_1
ΔE_2
ΔE_3
ΔE_4
ΔE_5
ΔE_6
ΔE_7
The average width $\langle X_i \rangle$
50
40
30
20
10
0
-0.6
-0.3
0.0
0.3
0.6
0.9
Strain s_{33} (%)
X_0
X_1
X_2
X_3
X_4
X_5
X_6
X_7

Figure 4

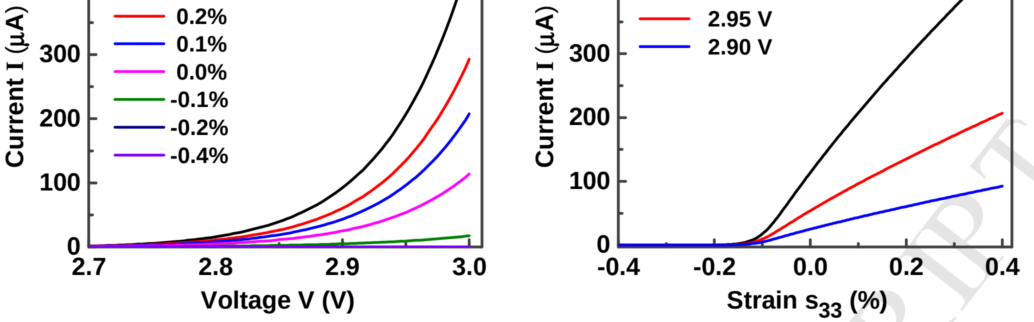
0.2%
0.1%
0.0%
-0.1%
-0.2%
-0.4%
Current I (μA)
Voltage V (V)
2.95 V
2.90 V
Current I (μA)
Strain s33 (%)

Figure 5

GaN	200 nm [49]	8 mm [50]	8 mm [50]	1.0 × $10^{[illegible]}$ [49]
AlGaN	2 nm [49]	8 mm [50]	8 mm [50]	1.0 × 10^{15} [49]
n-AlGaN	20 nm [49]	8 mm [50]	8 mm [50]	5.0 × 10^{18} [49]

devices.

2. The strain-induced piezoelectric field can effectively manipulate quantum state of 2DEG.

3. Piezoelectric field can enhance infrared photoelectric detection.